

Viscous vortex layers subject to general strain

K. Shariff*

NASA Ames Research Center

(Dated: December 23, 2024)

arXiv:2102.01266v1 [physics.flu-dyn] 2 Feb 2021

Abstract

Viscous vortex layers subject to a general linear strain are considered. They include Townsend's steady solution for plane strain (corresponding to a parameter $a = 1$) in which all the strain in the plane of the layer goes toward vorticity stretching, as well as Migdal's recent steady asymmetric solution for axisymmetric strain ($a = 1/2$) in which half of the strain goes into vorticity stretching. In addition to considering asymmetric, symmetric and antisymmetric steady solutions $\forall a \geq 0$, it is shown that for $a < 1$, i.e., anything less than the Townsend case, the vorticity inherently decays in time: only boundary conditions that maintain a supply of vorticity at one or both ends lead to a non-zero steady state. For $a > 1$, steady states require that opposite sign vorticity enter one or more boundaries. Only zero-integral perturbations of these states are stable; otherwise, the solution grows.

MOTIVATION

Vortex configurations subjected to a spatially linear strain flow can be used to model local regions of more complicated flows where the strain represents the local potential velocity induced by other vortex structures, typically of larger scale than the region being considered. Example solutions include Burgers' tubular vortex [1], Townsend's Gaussian vortex layer subject to plane-strain [2], and the celebrated Lundgren spiral which produces Kolmogorov's $k^{-5/3}$ energy spectrum [3–6]. It should be noted that Townsend's layer is unstable to the formation of concentrated tubular structures [7, 8].

Recently, Migdal [9] presented a steady asymmetric vortex layer solution for the case of axisymmetric strain ($a = 1/2$ below). In this solution the vorticity decays algebraically on one side of the layer and as a Gaussian on the other. It was the desire to interpret this solution that led to the present note. We conclude that in this configuration, stretching cannot keep up with diffusion unless there is a supply of vorticity from the algebraically decaying side. The symmetric solution, which Migdal did not consider, corresponds to algebraic decay on both sides, while the antisymmetric solution corresponds to annihilation of vorticities of opposite sign. The above conclusions apply equally well for values of $0 < a < 1$, though less and less of a supply of vorticity is needed as $a \rightarrow 1$ (for the symmetric and asymmetric steady solutions). For $a = 1$ we have Townsend's plane strain case in which a steady state is reached with zero boundary conditions on both sides and non-zero integrated vorticity in

the initial condition. For $a > 1$, steady states exist with inflow of opposite sign vorticity at one or both ends. Only zero integral perturbations of these states relax back to the steady state; otherwise, they grow.

ANALYSIS

We consider the unidirectional shear flow and associated vorticity

$$u_x = S(z, t), \quad \omega_y(z, t) = S'(z) \equiv G(z, t), \quad (1)$$

subjected to the irrotational strain

$$\vec{u}_{\text{strain}} = \alpha ((1 - a)x\vec{e}_x + ay\vec{e}_y - z\vec{e}_z). \quad (2)$$

The form (2) is general in principal coordinates: since the coefficients must add up zero (due to incompressibility), there are two free parameters, α and a .

We choose $\alpha, a > 0$ since to counteract diffusion we want a compression in z and stretching along y . For $a = 0$ all of the straining in the plane (xy) of the layer goes into advection and none into vortex stretching. For $a = 1/2$ we get Migdal's case of axisymmetric strain in which half of the straining goes into vorticity stretching and half into advection. For $a = 1$ we recover Townsend's case of strain in the yz plane (independent of x). In this case, *all* of the straining flow in the plane of the layer goes into vorticity stretching. The case $a > 1$ corresponds to even greater y stretching than Townsend's case and has compression along x .

The only non-trivial component of the vorticity equation is the y -component and it gives the PDE:

$$\partial_t G - \alpha z \partial_z G = a\alpha G + \nu \partial_{zz} G, \quad (3)$$

where ν is the kinematic viscosity. The second term on the left side of (3) represents advection while the first term on the right side represents stretching. Setting the time derivative equal to zero gives the ODE:

$$\nu G''(z) + \alpha z G'(z) + a\alpha G(z) = 0, \quad (4)$$

whose general solution given by Mathematica is

$$G(z, a) = c_1 G_1(z, a) + c_2 G_2(z, a). \quad (5)$$

If we define

$$\eta = \frac{z}{\sqrt{2\delta}} \text{ with } \delta \equiv (\nu/\alpha)^{1/2} \quad (6)$$

as a measure of the sheet thickness, then

$$G_1(\eta, a) = \exp(-\eta^2) H_{a-1}(\eta), \quad (7)$$

$$G_2(\eta, a) = \exp(-\eta^2) {}_1F_1\left(\frac{1-a}{2}, \frac{1}{2}, \eta^2\right). \quad (8)$$

The function ${}_1F_1$ is Kummer's confluent hypergeometric function and H_{a-1} is a Hermite function defined as

$$H_{a-1}(\eta) = 2^{a-1} \sqrt{\pi} \left[\frac{1}{\Gamma\left(\frac{2-a}{2}\right)} {}_1F_1\left(\frac{1-a}{2}, \frac{1}{2}, \eta^2\right) - \frac{2\eta}{\Gamma\left(\frac{1-a}{2}\right)} {}_1F_1\left(\frac{2-a}{2}, \frac{3}{2}, \eta^2\right) \right]. \quad (9)$$

The first term in G_1 (from the first term in eq. (9)) is proportional to $G_2(z; a)$, i.e., it is not linearly independent and we may discard it. However, since $G_1(z, a)$ as it stands is the solution (for $a = 1/2$) presented by Migdal [9], we shall not alter it.

Figure 1 plots $G_1(\eta, a)$ and $G_2(\eta, a)$ for various strain configurations. The two functions are asymmetric and symmetric, respectively. The asymmetry of $G_1(\eta, a)$ comes from the η in the second term of the Hermite function (9). Note that due to symmetry of the ODE (4) under $z \rightarrow -z$, a plus sign for the second term instead of the minus sign should be an equally valid solution, i.e, the mirror image of $G_1(\eta, a)$ should be an equally valid solution. While this can be achieved with a suitable choice of c_1 and c_2 , the $z \rightarrow -z$ symmetry is made more obvious if we use the pair of solutions

$$G^\pm \equiv \left[\frac{1}{\Gamma\left(\frac{2-a}{2}\right)} {}_1F_1\left(\frac{1-a}{2}, \frac{1}{2}, \eta^2\right) \pm \frac{2\eta}{\Gamma\left(\frac{1-a}{2}\right)} {}_1F_1\left(\frac{2-a}{2}, \frac{3}{2}, \eta^2\right) \right], \quad (10)$$

which are mirror images of each other. The functions $G^+ \pm G^-$ which are symmetric and antisymmetric, respectively, can also be used as a basis.

Consider a finite domain $\eta \in [-L, L]$. The case $a = 0$ corresponds to plane strain perpendicular to the vorticity so stretching is absent. To achieve a steady state in this case we need a source of uniform vorticity at one or both ends; for example, a vortex patch (see the $a = 0$ case in Figure 1a). As a increases one requires smaller boundary values until for $a = 1$ (Townsend), the required value is exponentially small in L^2 .

For the super-Townsend case ($a > 1$), refer to the curves for $a = 1.25$ in Figure 1. The symmetric and asymmetric steady solutions show opposite sign vorticity entering one or both

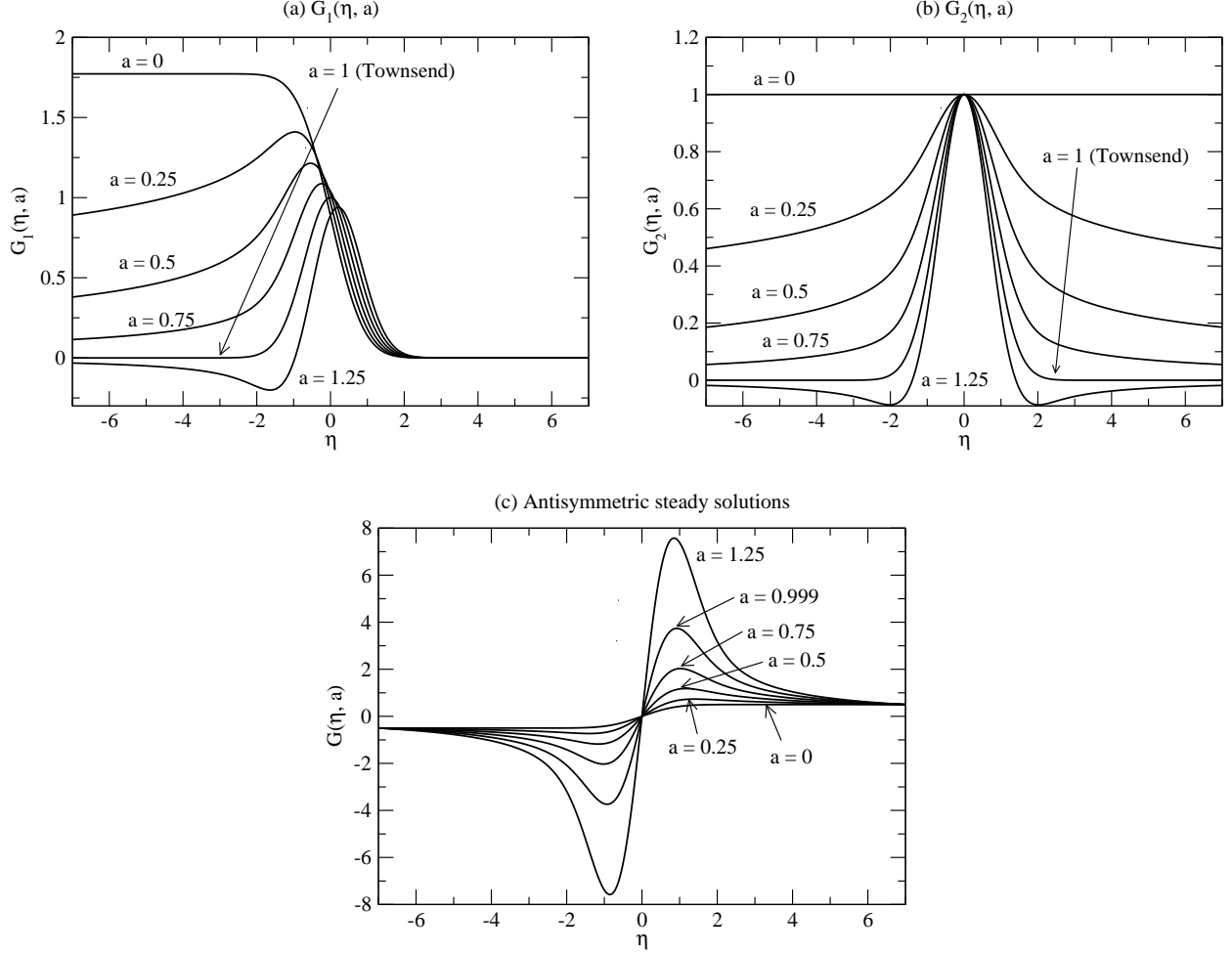


FIG. 1. (a) and (b) Two linearly independent solutions, $G_1(\eta; a)$ and $G_2(\eta; a)$ to the ODE (4) plotted for various strain configurations a . (c) Antisymmetric solutions constructed from a suitable linear combination of $G_1(\eta)$ and $G_2(\eta)$.

boundaries and changing sign before reaching $\eta = 0$. Since neither advection, stretching, nor dissipation can change the sign of the vorticity, to achieve such a steady state requires special initial conditions; this will be discussed in more detail in the next section.

The functions $G_1(\eta)$ and $G_2(\eta)$ may be combined to form antisymmetric solutions; see Figure 1c. One can do this for all a except $a = 1$ because $G_1(\eta, 1) \propto G_2(\eta, 1) = \exp(-\eta^2)$. This is why in Figure 1c the solution for $a = 0.999$ is plotted instead. However, since one can let $a \rightarrow 1$ arbitrarily closely, an antisymmetric solution does exist in the limit. To confirm this, the unsteady code was run for $a = 1$, an initial condition of zero, and antisymmetric boundary conditions $G(-7) = -0.5$ and $G(7) = 0.5$. The solution converged to a solution

as $t \rightarrow \infty$.

TIME-DEPENDENT BEHAVIOR

The unsteady linear PDE (3) was solved numerically. Since there are dimensions of length and time, we are free to set $\alpha = 2\nu = 1$ which makes $z = \eta$. The remaining parameters are the strain configuration a and those that involve the initial and/or boundary values of the vorticity. Denoting the peak magnitude of the vorticity at any instant as $|\omega|_{\max}(t)$, a time-dependent Reynolds number may be defined as

$$\text{Re} \equiv \frac{|\omega|_{\max}(t) \delta^2}{\nu} = |\omega|_{\max}(t), \quad (11)$$

for our choice of units. Since the problem is linear and amplitudes don't matter, there is no Reynolds number dependence.

The domain is $\eta \in [-L, L]$ with $L = 7$ and various Dirichlet boundary conditions are applied.

Figure 2 is for axisymmetric strain ($a = 1/2$) and panel (a) shows relaxation to the exact asymmetric steady state of Migdal [9] with an initial condition of zero and asymmetric boundary conditions $G(-7) = 0.5$ and $G(7) = 0$. Keeping in mind that there is advection of vorticity toward the origin, we see that, to maintain Migdal's asymmetric solution, one needs a continual supply of vorticity at one end; otherwise, the solution would eventually decay to zero. Figure 2b shows that the solution decays if conditions of zero are applied at both ends. Panel (c) shows relaxation to the symmetric solution with a symmetric supply of vorticity at both ends. Figure 2d shows relaxation to the antisymmetric solution in which vorticity of opposite sign enters the domain, is amplified by stretching and then annihilates.

Finally, we turn attention to some super-Townsend cases (Figure 3, $a = 1.5$). We begin with homogeneous boundary conditions $G(-7) = G(7) = 0$. For this case there is only the trivial steady solution $c_1 = c_2 = 0$ and so we expect that an unsteady solution will either decay or grow when starting from an arbitrary initial condition. Panel (a) shows that with an initial condition consisting of three half-cosines, the vorticity grows exponentially as a near-Gaussian. It grows in the negative direction because the initial condition has a negative integral. The corresponding Townsend case ($a = 1$) would saturate to a near-Gaussian

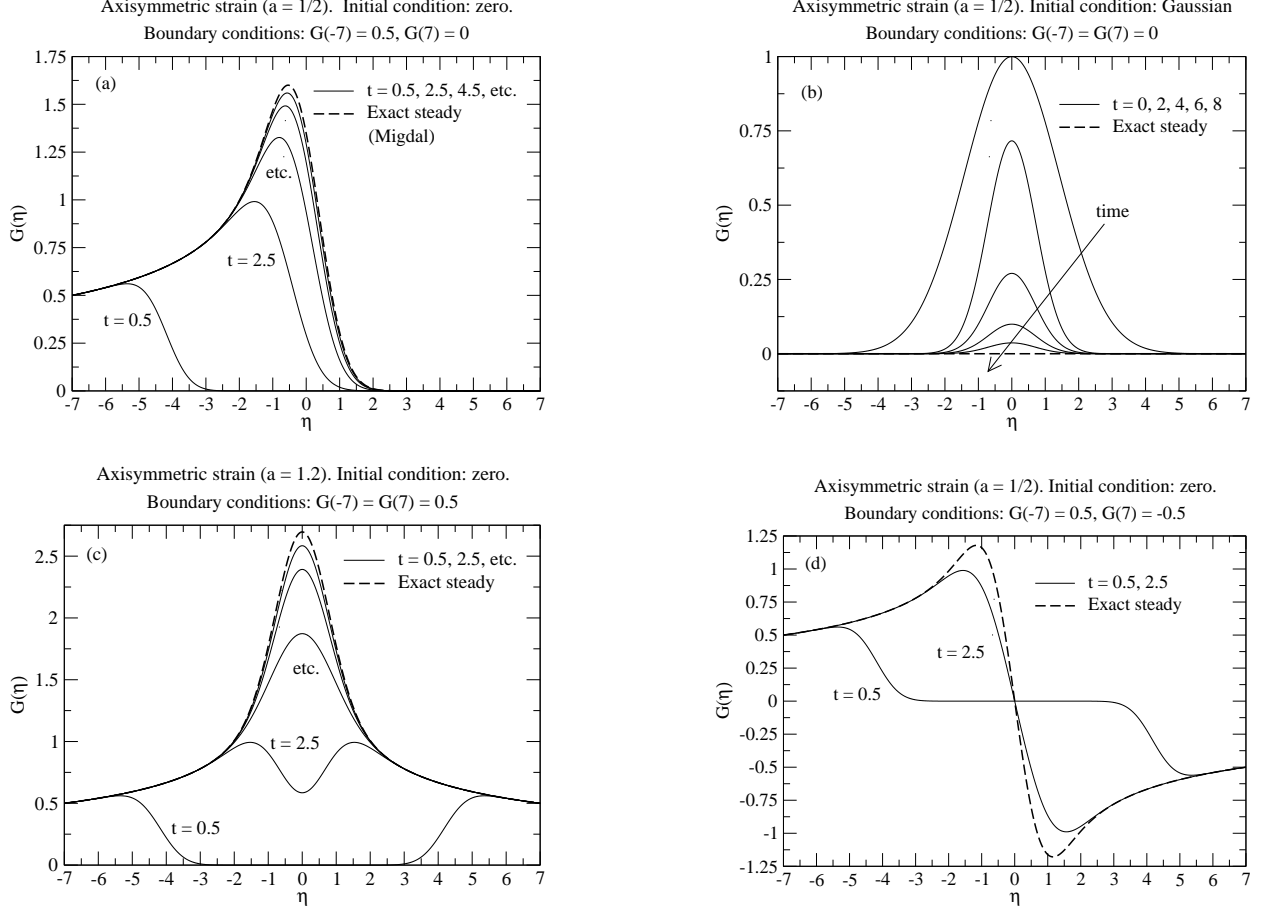


FIG. 2. Four axisymmetric strain cases ($a = 1/2$). (a) Relaxation to Migdal’s [9] asymmetric steady state with supply of vorticity at the left end. (b) Decay to zero with no supply at either end. (c) Relaxation to a symmetric solution with symmetric supply at both ends. (d) Relaxation to antisymmetric steady-state with supply of positive and negative vorticity followed by annihilation.

steady state. On the other hand, the sine wave initial condition,

$$G(\eta, 0) = -\sin(2\pi\eta/\lambda), \quad \lambda = 2L, \quad (12)$$

which has zero integral, decays to zero (Figure 3b). Next, we make a slight change by adding a small linear function, 0.01η , to (12) and enforce the compatible (antisymmetric) boundary conditions $G(\pm 7) = \pm 0.07$. In this case there is a non-trivial solution for c_1 and c_2 and the solution relaxes to the corresponding steady state (Figure 3c).

The next case is very instructive (Figure 3d). The initial condition is zero and symmetric negative boundary conditions are applied: $G(-0.5) = G(0.5) = -0.5$. The steady solution compatible with the boundary conditions is shown as the dashed line. It is obviously not

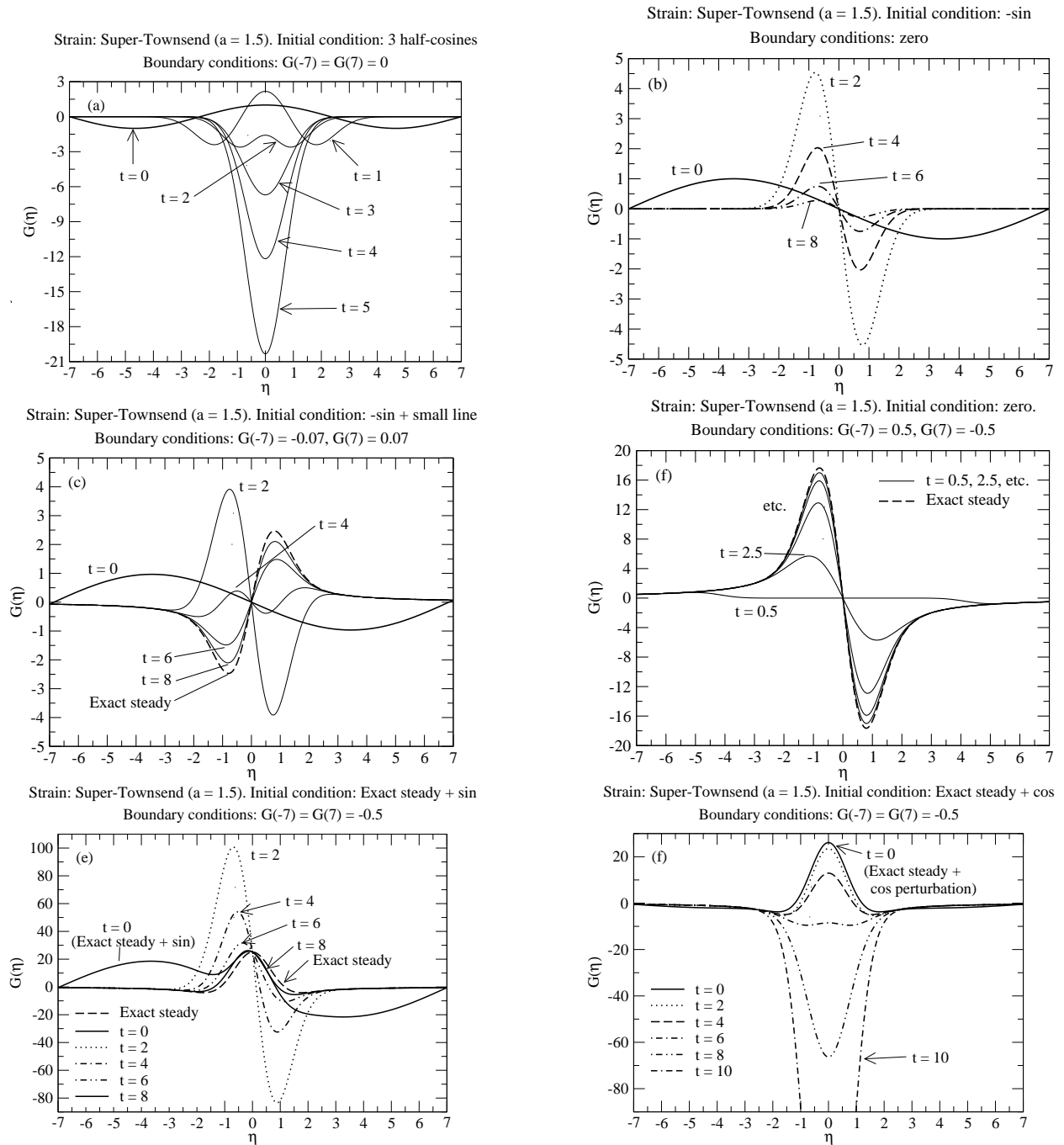


FIG. 3. Super-Townsend cases $a = 1.5$: (a) Exponential growth of negative vorticity with three half-cosine initial condition and zero boundary conditions. (b) Decay with a sine wave initial condition and zero boundary conditions. (c) Adding a small line to the sine wave leads to relaxation to the steady solution. (d) Failure to relax to the steady solution. (e) Relaxation back to the steady state after a conservative perturbation. (f) Failure to relax back to the steady state after a non-conservative perturbation.

reached as $t \rightarrow \infty$; instead negative vorticity grows exponentially. Why? In each half of the layer, $\eta < 0$ say, the steady solution has vorticity of both signs. To reach the steady state, vorticity must change sign after it enters the left boundary and flows toward $\eta = 0$ (recall that we started with no vorticity in the domain). However, neither advection, stretching, nor diffusion can change the sign of the vorticity. To reach the steady solution requires that the initial condition already contain the precise amount of vorticity of the opposite sign. To see this, consider Figure 3e where we started with the exact steady solution and applied one period of a sine wave as a perturbation:

$$G(\eta, t = 0) = G_2(\eta, a = 1.5) - 20 \sin(2\pi\eta/\lambda), \quad \lambda = 2L. \quad (13)$$

The perturbation has zero area and so does not change the total vorticity. As a result, the solution relaxes back to the steady solution. On the other hand, in Figure 3f, the perturbation has non-zero area: it consists of three half-cosines:

$$G(\eta, t = 0) = G_2(\eta, a = 1.5) + \cos(2\pi\eta/\lambda), \quad \lambda = 2L/3, \quad (14)$$

and does not disturb the boundary conditions. Note that the perturbation has more negative than positive area; the solution is unstable and negative vorticity grows exponentially. It was verified that when the sign of the perturbation was changed, positive vorticity grew exponentially. The results of the last two panels, (e) and (f), can be understood as follows. Since the problem is linear, we may consider the evolution of the perturbation separately under homogeneous Dirichlet boundary conditions and that was already done in Figures 3a and b. There we saw that an initial condition with zero total vorticity decays while an initial condition with a non-zero total vorticity grows.

I thank Prof. A. Migdal for sending me his manuscript and for his encouragement. Drs. I. Kiviashvili and A. Wray performed the internal review for which I am grateful. The data that support the findings of this study are available from the author upon reasonable request.

* Karim.Shariff@nasa.gov

- [1] J. Burgers, A mathematical model illustrating the theory of turbulence, in *Advances in Applied Mechanics*, Vol. 1 (Elsevier, 1948) pp. 171–199.
- [2] A. Townsend, On the fine-scale structure of turbulence, Proc. Roy. Soc. Lond. Ser. A. **208**, 534 (1951).
- [3] T. S. Lundgren, Strained spiral vortex model for turbulent fine structure, Phys. Fluids **25**, 2193 (1982).
- [4] A. Gilbert, A cascade interpretation of Lundgren’s stretched spiral vortex model for turbulent fine structure, Phys. Fluids A **5**, 2831 (1993).
- [5] D. Pullin and P. G. Saffman, On the Lundgren-Townsend model of turbulent fine scales, Physics of Fluids A **5**, 126 (1993).
- [6] D. Pullin, J. Buntine, and P. Saffman, On the spectrum of a stretched spiral vortex, Phys. Fluids **6**, 3010 (1994).
- [7] S. J. Lin and G. M. Corcos, The mixing layer: deterministic models of a turbulent flow. Part 3: The effect of plane strain on the dynamics of streamwise vortices, J. Fluid Mech. **141**, 139–178 (1984).
- [8] T. Passot, H. Politano, P. Sulem, J. Angilella, and M. Meneguzzi, Instability of strained vortex layers and vortex tube formation in homogeneous turbulence, J. Fluid Mech. **282**, 313–338 (1995).
- [9] A. Migdal, Asymmetric vortex sheet, Phys. Fluids (2021), Submitted. Preprint: arXiv:2101.06918v1 [physics.flu-dyn].